PROCEEDINGS OF SPIE

SPIEDigitalLibrary.org/conference-proceedings-of-spie

Plasma accelerator-based ultrabright x-ray beams from ultrabright electron beams

Ahmad Fahim Habib, Paul Scherkl, Grace Gloria Manahan, Thomas Heinemann, Daniel Ullmann, et al.

Ahmad Fahim Habib, Paul Scherkl, Grace Gloria Manahan, Thomas Heinemann, Daniel Ullmann, Andrew Sutherland, Alexander Knetsch, Michael Litos, Mark Hogan, James Rosenzweig, Bernhard Hidding, "Plasma accelerator-based ultrabright x-ray beams from ultrabright electron beams," Proc. SPIE 11110, Advances in Laboratory-based X-Ray Sources, Optics, and Applications VII, 111100A (9 September 2019); doi: 10.1117/12.2530976

SPIE.

Event: SPIE Optical Engineering + Applications, 2019, San Diego, California, United States

Plasma accelerator-based ultrabright x-ray beams from ultrabright electron beams

Ahmad Fahim Habib[a,b], Paul Scherkl[a,b], Grace Gloria Manahan[a,b], Thomas Heinemann[a,b,c], Daniel Ullmann[a,b], Andrew Sutherland[a,b,d], Alexander Knetsch[c], Michael Litos[e], Mark Hogan[d], James Rosenzweig[f], and Bernhard Hidding[a,b]

[a]Scottish Universities Physics Alliance, Department of Physics, University of Strathclyde, Glasgow G4 0NG, UK
[b]Cockcroft Institute, Sci-Tech Daresbury, Keckwick Lane, Daresbury, Cheshire WA4 4AD, UK
[c]Deutsches Elektronen-Synchrotron DESY, Hamburg 22607, Germany
[d]Center for Integrated Plasma Studies, University of Colorado Boulder, Boulder, Colorado 80303, USA
[e]SLAC National Accelerator Laboratory, Menlo Park, California 94025, USA.
[f]Department of Physics and Astronomy, University of California Los Angeles, Los Angeles, California 90095, USA.

ABSTRACT

We provide a pathway to compact ultrabright light sources, based on ultrabright, high energy electron beams emerging from a combination of plasma wakefield acceleration and plasma photocathodes. While plasma acceleration is known to produce accelerating fields three or four orders of magnitude larger than conventional accelerators, the plasma photocathode allows production of electron beams three or four orders of magnitude brighter than conventional, and thus is suitable to unleash the full potential of plasma accelerators. In particular, this is the case for various types of light sources, which profit enormously from an increased electron beam brightness. Building on the recent first experimental demonstration of the plasma photocathode, in this work we discuss the prospects of plasma photocathodes for key photon source approaches such as x-ray free-electron lasers, betatron radiation, ion-channel lasers and inverse Compton scattering.

Keywords: PWFA, plasma photocathode X-FEL, ICS, ICL, 6D brightness

1. INTRODUCTION

Electron beam-based light sources such as synchrotrons, Free-Electron Lasers (FELs), Inverse Compton Scattering (ICS) systems or Ion-Channel Lasers (ICLs) rely on high energy and high quality of the driving electron beam population. The electron beam needs to be compact in transverse and longitudinal phase space in order to radiate photons coherently when forced on undulating trajectories by an alternating magnetic field array in an undulator (FEL), by a laser pulse (ICS) or by plasma (betatron oscillations/ICL). They also need high energies in order to emit photons in the desired X-ray or γ-ray range. Plasma accelerators, both laser and particle-beam driven, produce accelerating fields which are three to four orders of magnitude larger than in conventional, metallic cavity and radiofrequency-based accelerator structures. Multi-GeV-scale, femtosecond-scale duration and kA-scale current electron bunches can today be routinely produced and accelerated by the large electric fields inside plasma waves driven either by a laser or charged particle beam, which expels plasma electrons transversely and excites a co-moving plasma accelerator cavity. The availability of such electron beams has nurtured their use as light sources; in fact, the construction and application of plasma-based light sources is a major R&D-driver.

Further author information: (Send correspondence to A.F.H. and B.H.)
A.F.H.: E-mail: ahmad.habib@strath.ac.uk, Telephone:+44 (141) 548 4726
B.H.: E-mail: bernhard.hidding@strath.ac.uk, Telephone:+44 (141) 548 4994

Advances in Laboratory-based X-Ray Sources, Optics, and Applications VII,
edited by Alex Murokh, Daniele Spiga, Proc. of SPIE Vol. 11110, 111100A
 · doi: 10.1117/12.2530976

However, likewise crucial are production of low energy spread and emittance electron beams to realize compact transverse and longitudinal phase spaces, respectively. Regarding energy spread, the large electric field *gradient* inside a plasma cavity, ranging e.g. from +50 GV/m at the front of a 100 μm-scale plasma bubble/blowout structure to -50 GV/m at its end, implies that even for injected electron beams of few fs duration, the head of the beam will see substantially different accelerating fields than the tail. This leads to a correlated energy chirp and thus increased longitudinal phase space, which can be a showstopper for achieving lasing in an FEL. With respect to emittance, the fact that the plasma wave driver beam kicks out plasma electrons transversely, and their re-attraction by immobile plasma ions – the very essence of plasma accelerators – in turn means that the transverse momentum of these plasma electrons, which may be captured in the plasma wave in conventional injection methods, is large. This sets limits on the compactness of the transverse phase space and emittance of electron beams produced by such conventional injection methods. Likewise, similar to the energy spread considerations, a too large emittance will not allow achieving lasing in an FEL at given electron energy. The key beam parameters, current, energy spread, and emittance are combined in the crucial composite parameter brightness, which scales linearly with the current, inversely with the emittance in each plane and the energy spread. The central importance of brightness e.g. for free-electron-lasers[1] is well known, because, for example, it defines the gain of the photon field in an FEL. Reduction of emittance and energy spread are therefore top priorities in the development of plasma-based accelerators, as they currently present a roadblock for the full exploitation of plasma accelerators for light sources.

2. THE PLASMA PHOTOCATHODE: PRODUCTION OF ULTRAHIGH BRIGHTNESS ELECTRON BEAMS WITH PLASMA WAKEFIELD ACCELERATORS

The key requirements discussed in the introductory section are very challenging to meet, however they are not unsurmountable. Electron beam-driven plasma wakefield acceleration (PWFA) has evolved into an increasingly attractive approach and is now considered as feasible alternative for next generation particle accelerators. In addition to the enormous accelerating gradients, enabling tens of GeV energy gain per metre[2,3] in a dephasing-free fashion and thus providing a near-ideal plasma accelerator environment, a transformative thrust is added by the invention and development of plasma photocathodes. In this approach, also known as Trojan Horse technique, one relies on laser-based release of cold electrons instead of injection of hot, thermal plasma electrons.

The plasma photocathode[4,5] is an advanced plasma-based electron injector which allows releasing cold electrons directly inside a non-linear plasma wave. In principle, it can also be realized in Laser Wakefield Acceleration (LWFA) but manifests its advantages most pronounced in a beam-driven plasma wakefield accelerator. This is because of the favorable properties of PWFA, such as dephasing-free and dark current-free acceleration in a comparably robust acceleration cavity with fixed phase relation over a long acceleration distance, allowing multi-GeV energy gain in a single stage,[2,3] but characteristically also because unlike with LWFA, the peak electric fields of the PWFA driver beam are comparable to the magnitude (GV/m-scale) of the accelerating and focusing fields of the plasma wave. In contrast, state-of-the-art LWFA requires laser pulse drivers with electric peak fields many orders of magnitude larger (TV/m scale), which exceeds the tunneling ionization threshold of elements by orders of magnitude and thus imposes significant residual transverse momentum on plasma electrons in its path. In the Trojan Horse method, the comparably low peak electric fields of the PWFA driver can be below tunneling ionization thresholds and thus allow subsequent exploitation of laser-gated tunneling ionization just above the electric field thresholds for controlled injection of high quality electron beams. The plasma photocathode is realized as follows: a relativistic electron driver beam excites a non-linear plasma wave with its typical "blowout"-like structure in a (laser-)preionized plasma such as hydrogen. A co-propagating, spatiotemporally aligned and synchronized laser pulse is then focused inside this blowout structure such that the laser pulse intensity only around the focal point exceeds the tunnel ionisation threshold of a hitherto non-ionized component, for example neutral background gas such as helium. The laser pulse then liberates helium electrons localized directly inside the blowout structure, where the GV/m-scale accelerating PWFA gradient accelerates those electrons rapidly to relativistic energies, thus counter-acting the space charge field of the injected electrons and preventing transverse phase space dilatation. Because of the relatively low intensities and vanishing ponderomotive potential of the plasma photocathode laser pulse, the transverse residual momenta of the released

electrons are negligible. Localized injection in conjunction with negligible transverse residual momentum results in extremely compact transverse phase space volume of produced electron populations, reflected by nm-rad-scale normalized emittances ϵ_n. This is a key advantage of this method, whereas tunneling ionization based methods in conventional LWFA systems require much higher laser intensities. This raises emittance to values typically of the order of micrometer rad (μrad), a similar level as obtainable for classical metallic cavity-based systems and three orders of magnitude larger than by the plasma photocathode injector. Combined with the intrinsic compression of electron populations released in plasma-based accelerators to fs-duration and associated kA-scale peak currents I_p, such ultralow emittance in both transverse planes yields ultrahigh 5D-brightness $B_{5D} = 2I_p/\epsilon_{n,x}\epsilon_{n,y}$, exceeding those obtainable from plasma-based and conventional accelerators by approximately up to six orders of magnitude.[6] Furthermore, in contrast to conventional methods of injection, the injection process in Trojan Horse is decoupled from the acceleration structure, which enables tuneability and controllability of the injected "designer" electron beams ("witness beams") by tuning the plasma photocathode laser parameters. This approach therefore addresses the challenge of electron beam quality enhancement in plasma-based accelerators as the above mentioned central obstacle towards potential light source applications e.g. via X-ray free-electron lasers (X-FEL), inverse-Compton scattering and ion-channel lasers. Recently, an experimental breakthrough has been achieved by the E-210: Trojan Horse collaboration at the Stanford Linear Accelerator (SLAC) Facility for Advanced Accelerator Experimental Tests (FACET), by demonstrating the feasibility of the plasma photocathode method for the first time.[7] This breakthrough, combined with the development of novel conceptual techniques for energy chirp compensation are very encouraging milestones towards laboratory-scale ultra-high brightness electron beam accelerators. The combination of ultra-high energy gain and ultra-high beam quality thus constitute game-changing advances which may allow, for example, driving future light sources with unique features, and other applications such as in high energy physics.

2.1 Generation of Ultrahigh 6D Brightness Electron Beams

Ultralow emittance, and correspondingly ultrahigh 5D brightness are key parameters for many applications utilizing particle accelerators. In addition, the energy spread of the produced electron witness beams is a crucially and equally important parameter. The enormous "sawtooth"-like shaped accelerating electric field gradient in plasma-based accelerators comes at the price of an intrinsic by-product, namely the inherent correlated energy spread (energy chirp) causing a time-energy correlation in the longitudinal phase space of a witness beam as shown in Fig. 1 (left). The energy chirp arises because the electric field at the head of the accelerated witness beam is substantially lower than at the tail, and consequently, the witness beam head has lower energy than the witness beam tail. This leads to the negative energy chirp typical to plasma wakefield accelerators. This deep-seated characteristic is generally detrimental as it can compromise or even prevent key applications such as X-FEL. Further, already the extraction of such chirped witness beams from the plasma accelerator stage will be more difficult, and electron beam transport optimization and matching may lead to significant quality degradation due to chromatic aberration effects.[8,9] The energy spread and chirp is indeed an important bottleneck and compensation ("dechirping") techniques are of paramount importance for the application of plasma-based accelerators.

A recent conceptual breakthrough[10] suggests that the energy chirp of a witness beam can be removed in a single plasma accelerator stage, without compromising the witness beam quality in terms of emittance, by means of tailored beam-loading[11,12] of a second high-charge electron beam which we call "escort beam". In proof-of-concept 3D Particle-In-Cell (PIC) simulations[10] performed with VSim,[13] a FACET-II-like[14] 10 GeV-energy electron beam sets up a typical dephasing-free PWFA stage in a preionized plasma channel of nominal density $n_0 = 1.1 \times 10^{17}\,\mathrm{cm}^{-3}$ corresponding to a plasma wavelength of $\lambda_p(\mu m) = 2\pi c \times 10^3(m_0\varepsilon_0/e^2 n_0(cm^{-3}))^{1/2} \approx 100\,\mu m$, where c is the speed-of-light, m_0 is the electron mass, e and ε_0 are the electron charge and the electric constant, respectively. Its charge density $n_d = N_d/[(2\pi)^{3/2}\sigma_z\sigma_r^2]$ is optimized such that the dimensionless beam charge[15] $\tilde{Q} = (2\pi)^{3/2}(n_d/n_0)\sigma_z\sigma_r^2 k_p^3$ exceeds the blowout condition $\tilde{Q} > 1$, where N_d is the total number of electrons in the driver beam, σ_z and σ_r are the driver beam longitudinal and radial dimensions, respectively, and $k_p = 2\pi/\lambda_p$ is the inverse plasma skin depth. At the same time, it is ensured that the PWFA-stage can be operated dark-current-free[16] by avoiding unwanted hot spots within the effective trapping volume. Once the blowout structure is formed, a co-propagating, low intensity plasma photocathode laser pulse releases electrons with negligible transverse momentum directly within the blowout structure. The electric field accelerates the

witness beam quickly to relativistic energies W_{mean} in few millimetres, see Fig. 2 (solid black line). Because the space charge force decreases with γ^{-2}, where γ is the relativistic Lorentz factor associated with the beam energy, space charge induced emittance degradation effects are quickly suppressed. The initial nm rad-scale electron beam emittance produced by the plasma photocathode release process therefore can be largely preserved, which in turn allows production of electron beams of very high quality and energy. At a later stage of witness beam acceleration, for the same γ^{-2}-scaling, its emittance is further "relativistically stabilized". Now, a second electron beam population can be released, for example by a second plasma photocathode, which liberates a high charge density escort beam n_{b} such that it spatially overlaps with the witness beam when trapped. The charge density of the escort beam shall be sufficiently high to overload the wakefield at the witness beam trapping position, thus flipping its local gradient. Now, the witness beam head is accelerated at a higher rate than the witness beam tail, as predicted by a simplified 1D cold-fluid model in Fig. 1 (right). This reversed accelerating gradient induces a counter-clockwise rotation of the longitudinal phase space of the witness beam and consequently, the energy spread ΔW_{rms} decreases with the propagation distance. Fig. 2 (left) depicts the evolution of the energy spread ΔW_{rms} during the acceleration, characterized by a decreasing energy spread after the escort beam is released. The witness beam energy spread is minimized to $\Delta W_{\mathrm{rms,min}} = 2.56\,\mathrm{MeV}$ at the acceleration distance $z_{\mathrm{acc}} = 2.4\,\mathrm{cm}$ at a mean energy of $W_{\mathrm{mean}} \approx 774\,\mathrm{MeV}$. After this point, the energy spread increases because the witness beams starts accumulating positive energy chirp.

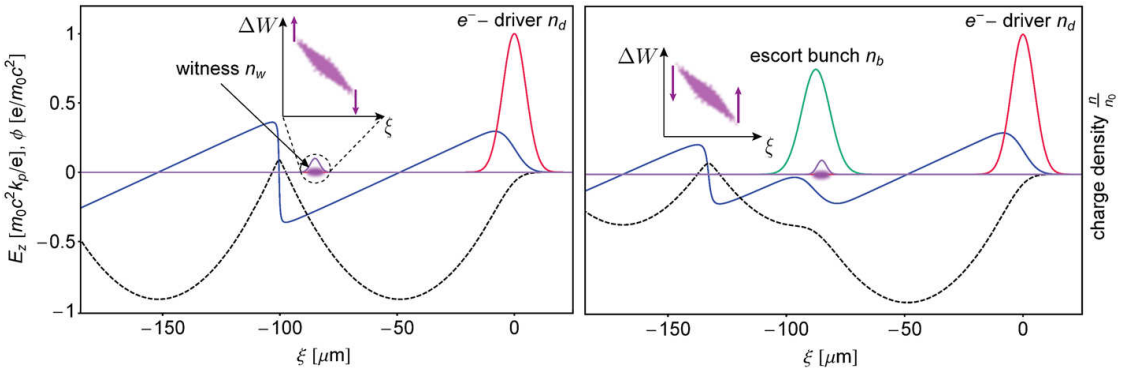

Figure 1. Semi-analytical solution of the electrostatic wake potential exited by an electron beam driver in a 1D cold fluid model. A Gaussian charge distribution driver beam (red solid line) propagates to the right and excites a parabolic electrostatic wake potential (black dashed line) resulting in a saw-tooth shaped plasma wakefield (solid blue line). In the left panel, a low charge witness beam (purple) is loaded into the back of the wake and accumulates the typical negative energy chirp during its acceleration, indicated by the longitudinal phase space inset (purple). In the right panel, a high charge escort beam (solid green line) is additionally trapped at the witness beam position and overloads the wakefield such that the witness beam head is accelerated stronger than its tail, which manifests in counter-clockwise longitudinal phase space rotation. The black dashed line shows the electrostatic potential which gives rise to the longitudinal wakefield. Data adapted from Ref. 10.

Fig. 2 (right) shows the corresponding witness beam longitudinal phase space at the optimum dechirping point with key slice parameters along the bunch. Because the energy chirp is removed completely from head to tail, the projected relative energy spread of $\Delta W_{\mathrm{rms,min}}/W_{\mathrm{mean}} \approx 0.3\,\%$ is very close to the counterpart mean slice energy spread $(\Delta W_{\mathrm{rms,min}}/W_{\mathrm{mean}})_{\mathrm{slice}} \approx 0.26\,\%$. The normalized emittance of the witness beam population is unaffected by the dechirping method, hence, the ultrahigh 5D-brightness combined with the minimized energy spread leads to unprecedented ultrahigh 6D-brightness beam $B_{6\mathrm{D}} = B_{5\mathrm{D}}/0.1\%\Delta W_{\mathrm{rms,min}}/W_{\mathrm{mean}} \approx 5.5 \times 10^{17}\,\mathrm{A/m^{-2}}/0.1\%\mathrm{bw}$. The remaining residual energy spread $\Delta W_{\mathrm{rms,min}} \simeq \Delta W_{\mathrm{res,max}}$ obtained in this simulation can be further reduced by decreasing the ionisation volume with smaller laser spot sizes and operation at lower plasma wave medium densities n_0, because in the first order approximation the absolute energy spread scales as $\Delta W_{\mathrm{res,max}} \propto w_0^2\sqrt{n_0}$;[10] this scaling has been confirmed in Ref. 17. Although computationally more costly to simulate, experimentally such operation at lower plasma densities is in many ways easier as it naturally improves the spatiotemporal precision of injection. At higher witness beam energies, the relative energy spread will be further reduced because of the adiabatic damping with the energy $\Delta W_{\mathrm{res,max}}/W_{\mathrm{mean}}$. This can be simply

achieved by releasing the escort beam at the later stage of the acceleration.

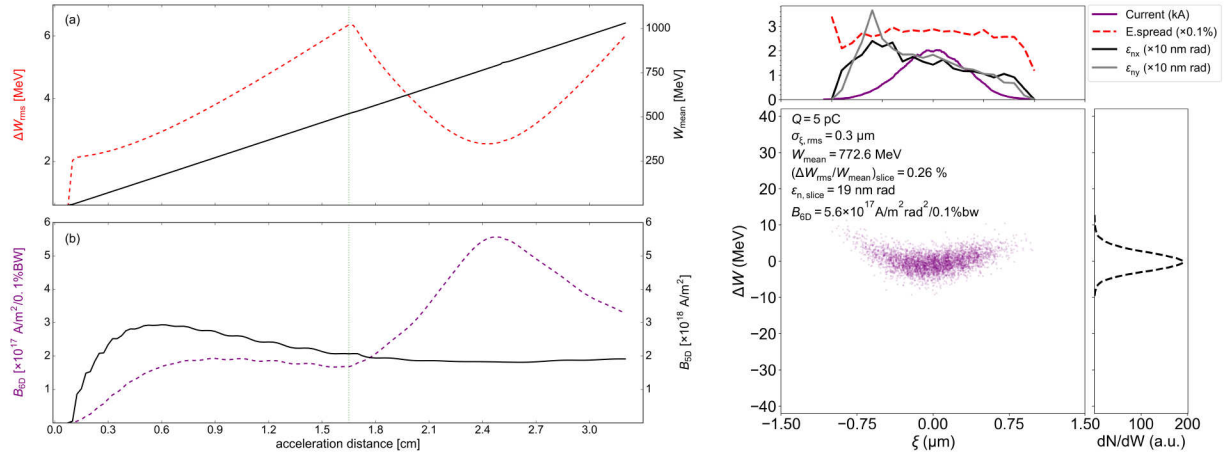

Figure 2. Witness beam parameter evolution during acceleration and dechirping as function of acceleration distance, and the longitudinal phase space at the optimum dechirping point, extracted from 3D Particle-In-Cell simulation with VSim. In the left top panel, the witness beam energy spread (red dashed line) W_{rms} and energy gain (black solid line) W_{mean} evolution is shown. The escort beam is released at the vertical green dashed line, which triggers dechirping until the witness beam energy spread decreases to a minimum at $z_{\mathrm{acc}} = 2.4\,\mathrm{cm}$, after which it increases because of the positive energy chirp it now develops. Note that the energy gain continues during the whole process. In the left bottom panel, the corresponding 6D brightness (dashed purple line) and 5D brightness (solid black line) of the witness beam are depicted. The 6B brightness is peaking at the optimum dechirping while the 5D brightness stays unaffected because the emittance of the witness beam is preserved during the dechirping process, and 5D brightness is not energy dependent. In the right hand side of the figure, the dechirped witness beam longitudinal phase space is shown with key beam slice parameters (top panel) and the spectral density (right panel). Data adapted from Ref. 10.

This energy chirp compensation method enables accurate control over the longitudinal phase space of the otherwise ultrahigh 5D-brightness witness beam in the same acceleration stage. It applies a further level of decoupling and flexibility, allowing to transform the ultrahigh 5D-brightness of plasma-photocathode-generated electron beams into beams with unprecedented 6D-brightness. While it is expected that the approach will develop highest impact in context with ultrahigh 5D-brightness witness beams from plasma photocathodes, the method is a general one. In principle, it can be utilized with witness beams from different injection methods in PWFA as well as in LWFA, or even for externally injected ones. It further contains intrinsic stabilisation properties which makes it resilient against jitter of the release plasma photocathode laser pulse .[18] Additionally, the flexibility of independently tuneable plasma photocathode laser pulses allows serving different purposes in the same acceleration stage. For example, it can also allow dechirping of multiple electron beams of different energies and properties[19] in the same plasma cavity, or generation of beams with widely arbitrary energy chirps, e.g. positive energy chirp. This is an intrinsic consequence of decoupling the witness bunch injection process from the accelerating structure and from the escort beam based chirp control in a single ultralow emittance stage, and the far-reaching capabilities this opens. In contrast to other methods of dechirping which rely on multiple stages and a reduction of energy chirp due to self-driven plasma wakefields[20–22] similar to e.g. dielectric wakefield dechirpers such as used at LCLS, the method described in Ref. 10 and above uniquely is compatible with lowest emittance and highest 5D-brightness beams. The capability to work with nmrad-scale emittance beams instead of μmrad-scale beams as used in Ref. 20–22 is a key advantage indeed, in particular for light source applications.

It is also important to point out that tailored beam loading can of course also be achieved directly by the witness release process itself, as production of higher charge can be obtained e.g. by ramping up the helium gas density or by increasing the plasma photocathode laser pulse energy. However, although the acceleration is rapid and space charge forces are quickly suppressed, there is a non-negligible space charge-induced emittance growth resulting in notable decrease of 5D brightness, which due to the quadratic scaling with emittance cannot be compensated by the potentially higher current values at higher bunch charge. While this method of a single

plasma photocathode and tailored beam loading for low energy spreads is thus capable to produce sub-micron emittance values in both planes, the lowest emittance values and highest 6D brightness values are obtainable from the escort beam method. We foresee the single-bunch beam-loading plasma photocathode as an intermediate regime and simplified pathway to be realized e.g. as a milestone for plasma-based hard X-ray FEL's.

2.2 E210: Experimental Demonstration of Plasma Phothocathode PWFA at SLAC FACET

The Stanford Linear Accelerator Center hosted a dedicated test facility for novel and advanced plasma wakefield acceleration experiments called FACET. At SLAC, pioneering R&D work has been conducted in advanced plasma accelerator concepts since the 1990's with many experimental breakthroughs in PWFA. These breakthroughs include, for example, demonstration of multi-GeV energy gain in PWFA,[2] high efficiency acceleration of an electron bunch in PWFA,[3] acceleration of positrons in a self-loaded PWFA,[23] and positron acceleration in a hollow plasma channel.[24] In 2011/12, the "E-210: Trojan Horse PWFA" undertaking was approved as a proof-of-principle experiment for FACET, aiming to explore and demonstrate the feasibility of the plasma photocathode concept. SLAC FACET is an ideal test facility for PWFA, as the accelerator provides high current electron beams, suitable for driving strong, non-linear plasma wakes. The combination of suitable experimental environment and the added installation of a synchronized laser system for preionization and plasma photocathode capability, PWFA expertise at FACET, and extensive in-depth theoretical and experimental work by academics and researchers from a multi-national collaboration mainly from Europe (University of Strathclyde, University of Hamburg, DESY, University of Oslo) and the US (RadiaBeam Technologies, UCLA, RadiaSoft, University of Colorado Boulder, University of Texas at Austin, Tech-X) eventually allowed to unlock the plasma photocathode injection scheme experimentally.[7,14,25] This was realized in 90° geometry between electron driver beam axis and plasma photocathode laser pulse for reasons described below. This achievement marks a major milestone towards producing ultrahigh brightness electron beams in PWFA, has triggered the co-development of many auxiliary techniques e.g. for spatiotemporal alignment and synchronization of high-intensity beams and has comprehensively increased the confidence in feasibility and potential of the scheme.

The path towards successful demonstration of the plasma photocathode required the implementation and commissioning of various novel capabilities at FACET. For example, previous PWFA experiments at FACET utilized alkali vapour ovens where lithium or rubidium were self-ionized by the electric field of the driver electron beam to set up the plasma cavity. However, for more stable and efficient acceleration and plasma photocathode realization, a wide laser-preionized plasma channel based on more manageable media (e.g. noble gases) than aggressive alkali metals, is desirable, and the plasma photocathode injection naturally also requires an ionizing laser pulse for injection. A 10-TW scale Ti:Sapphire laser system was therefore installed and synchronized to the FACET linear accelerator for preionization, to power the plasma photocathode and for various diagnostics. A long plasma channel was attained by selectively ionizing hydrogen in the interaction chamber, flooded by a multi-component gas mixture consisting of hydrogen and helium, making use of the high-power fraction of the laser pulse. An axicon/axilens optic was implemented and has been tuned such that it tunnel ionized the hydrogen fraction of the gas to produce the plasma channel, while keeping the ambient background helium with its substantially higher ionization threshold in neutral state, such that it could be used for the injection laser pulse. The combination of hydrogen and helium is comparably straightforward to manage experimentally, and a key advantage of a flooded chamber approach is the easy optical access for diagnostics and injection. Ideally, the laser-preionized plasma channel should be wide enough to reliably sustain the blowout structure without plasma channel boundary effects for a stable and robust acceleration. Note that in ion-channel laser applications (see Sec. 3.3), it may be desirable to locally narrow down the the channel width in order to switch to the "wakeless" regime where acceleration of the witness beam is switched off. The huge electron driver beam density at FACET in excess of 10 kA is easily sufficient to support trapping of electrons released by laser triggered injection inside the plasma cavity even at low plasma wavelengths. However, the preionized plasma channel width was limited as result of the employed laser system, restrictions of spatial footprint of the setup and employed optics. Therefore, to fit the plasma cavity into the comparably thin plasma channel with a width of order of 100 μm, comparably large plasma densities ($n_0 \approx 10^{17}\,\mathrm{cm}^{-3}$) had to be used. At high plasma and large driver electron bunch densities, the electric fields around the drive beam as well as at the wakefield vertex are large. Only a small range of plasma densities permitted sufficiently large plasma cavities on the one hand, and avoidance of hot spots which would

lead to driver beam or wakefield ionization of helium[16] on the other hand, or at least to suppress trapping of such hot spot-generated sources of dark current. Operation at longer plasma wavelengths reduces the wakefield strength and hence enables safely to prevent potential wake ionization of helium. Longer plasma wavelengths also relax demands on synchronization and alignment between injection laser pulse and electron driver beam for stable operation, however in turn require plasma channels with larger diameter to accommodate the blowout structure. Hence, production of wide plasma channels for stable operation is one of the key technical challenges in PWFA in general.

In order to access the plasma photocathode injection scheme, a laser pulse perpendicular to the driver electron beam propagation axis in 90° geometry was spatiotemporally synchronized and aligned at fs and μm scale precision to the driver beam by means of a novel technology based on optically accessible plasma afterglow response. This method was supported and benchmarked by state-of-the-art methods of electro-optical sampling (EOS) for time-of-arrival (TOA) and bunch duration and spacing measurements. EOS was another capability which was first installed as part of the E-210 program, then crucially serving also other experiments such as for positron acceleration.

To achieve controlled laser-triggered injection into the PWFA, we first generated a plasma filament in the intersection region with the driver electron beam before its arrival by ionizing an approximately 100 micron-wide helium plasma filament with the laser pulse in the 90° geometry. When properly aligned, the associated plasma density spike then triggered density downramp injection – a concept long sought for in PWFA and here realized for the first time as part of E-210. This method is called "Plasma Torch" injection[26,27] and is an all-optical version of plasma density downramp injection which we used as a stepping stone towards the plasma photocathode injection method: by delaying the injection laser pulse arrival, and by reducing the laser pulse energy, we successively approached and entered the Trojan Horse mode.[7] Both related laser-triggered injection methods are tuneable and flexible, and constitute experimental firsts. A challenge specifically to the Trojan Horse method is the inherent shot-to-shot temporal jitter between the FACET linac-generated driver electron beam and the plasma photocathode laser pulse. This jitter arises in part from the thermal cathode used in the SLAC linac and the strong compression requirements to attain driver beam densities for $\tilde{Q} > 1$ to drive a nonlinear wakefield. Additionally, the limited plasma channel width introduced highly complex wakefield dynamics along the acceleration direction, and even wakefields which became decelerating during passage through the plasma .[7] The inadequate plasma channel width also amplified sensitivity to shot-to-shot jitters of preionization laser intensity, pointing etc., and driver electron beam and injector laser jitters. The small plasma blowout size with the comparably long electron driver beam, and the 90° geometry with the comparably long plasma photocathode laser pulse Rayleigh length, furthermore increase the emittance as explained e.g. in Ref. 7. These technical challenges will be addressed in upcoming experimental runs e.g. at FACET-II, aiming to realize the full reach of plasma photocathodes with regard to emittance and brightness. It is very encouraging, that even under suboptimal experimental boundary conditions at FACET both injection methods – Plasma Torch and Trojan Horse – could be clearly demonstrated.

2.3 Upcoming Experimental Challenges and Programmes

The E-210: Trojan Horse PWFA experimental programme at FACET has demonstrated feasibility of the plasma photocathode technology, and has established pathways on how to realize them experimentally. However, experimental boundary conditions such as drive beam and injector laser beam jitter and limited preionized channel width restricted the accessible parameter range and stability of electron beam output substantially. These restrictions are well understood and evaluated. The lessons learned have significantly contributed to the design of FACET-II to resolve these restrictions, for example, by implementing state-of-the-art photocathode electron gun to produce the driver beam.[14] We developed various methods and techniques which address and allow to overcome the limitations of previous experiments in the future.[7,14,25] The flagship experiment for this at FACET-II is the "E-310: Trojan Horse-II" collaboration, dedicated to explore and realize the full potential of the Trojan Horse scheme, and to realize tunable "designer" electron bunches with nm-rad scale emittances and associated brightness orders of magnitude better than state-of-the-art. This can be obtained by operating at substantially reduced plasma wavelengths and/or by using shorter plasma photocathode laser Rayleigh lengths or methods such as simultaneously space-time focused laser beams[18] or similar techniques to confine the "effective" Rayleigh length of the laser beam, and/or by moving towards smaller angles between driver particle beam and

plasma photocathode laser beam in (near-)collinear or (near-)countercollinear geometry. This will profit from significantly improved plasma channel width and increased stability of the FACET-II driver and laser beams. In particular, realizing a wider plasma channel (see Fig. 3 (left)) will allow operation at lower plasma densities, corresponding to longer plasma wavelength. This relaxes not only the timing and alignment requirements of plasma photocathode injection but also enables to access electron beams of very low energy spreads, potentially down to $\Delta W_{\mathrm{rms}}/W_{\mathrm{mean}} \approx 0.01\,\%$ level[10] (see Fig. 3 (right)).

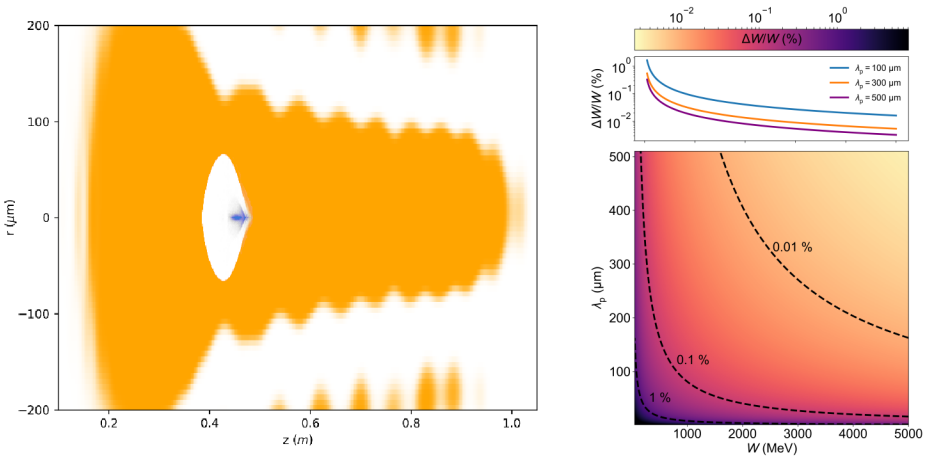

Figure 3. Left panel: A much wider plasma channel (orange) than in E-210, thus being able to accommodate a much longer plasma wavelength PWFA-structure (white), driven by a FACET-II sized electron beam (blue) propagating to the right. Right panel: Longer plasma wavelengths λ_{p} allow the plasma photocathode to generate electron beams with smaller absolute energy spreads, based on a scaling law from Ref. 10, which allows reaching sub-0.01% relative energy spreads already at few GeV electron energies, which are today routinely reached by modern plasma accelerators in single stages.

The Plasma Torch (optical density downramp) method is an injection method in its own right, capable of generating high brightness electron beams with very relaxed timing requirements compared to the Trojan Horse scheme. The experiment "E-311: Plasma Torch Optical Density Downramp Injection" at FACET II will be dedicated to investigate the capabilities of the Plasma Torch injection in its full extent, including unique capabilities such as asymmetric and confined density spikes with extreme gradients and shapes. Plasma Torch injection studies will also benefit from the SLAC linac photocathode upgrade and improved plasma channel generation. Injection processes will be studied systematically by changing injector laser properties and exploiting their influence on the downramp properties and the trapping process. As in E-210, the plasma torch downramp injection will also serve as a stepping stone (E-311) towards plasma photocathode (E-310) realization, but also can form a building block for the "E-313: Multibunch dechirper for ultrahigh 6D brightness beams" experiment. This experiment aims at production of multi-bunches[19] and the production of chirp-controlled ultrahigh brightness electron beam populations by exploring "escort"-beam dechirping of single or multiple high-5D-brightness beams, and thus production of ultrahigh 6D-brightness electron bunches. Further, experiments such as "E-315: Plasma afterglow attosecond metrology" and "E-316: Icarus – Transient tunneling ionization of crossing laser and electron beams" will be further developing novel diagnostic methods for extremely dense electron and positron beam metrology, synchronization and alignment. In conjunction, the FACET-II experiments E-310–E-317 aim at a comprehensive step change of high quality electron beam production and their diagnostics.

Complementary to FACET-II, other linac-PWFA based facilities such as at DESY FLASHForward, INFN SPARC_LAB (foreseen as main PWFA arm of EuPRAXIA), CLARA Full Energy Beam Exploitation (FEBE), are also emerging opportunities for relevant PWFA experiments, such as plasma torch density downramp injection and potentially even plasma photocathode realizations, if the driver beam current threshold of approximately 6 kA for straightforward Trojan Horse injection can be achieved at these installations, or by using auxiliary techniques such as density downramp assisted plasma photocathode injection[28] to relax the trapping threshold.

Due to its unique capabilities, in particular the huge driver currents which allow scanning of most advanced injection schemes over comprehensive parameter ranges, the role of FACET-II therefore is once again a fundamental pioneering one over the next years. It is extremely important for further fundamental work and prototyping of the plasma photocathodes as standardized approach, which can be then be widely implemented, for example also to boost the brightness of existing FEL facilities, for example at LCLS, LCLS-II (see Fig. 4), and European XFEL, in energy and brightness afterburner transformer modes. Next to exploratory machines such as FACET-II and such afterburner systems, and high-repetition rate linear accelerators dedicated to plasma photocathode PWFA, there is a further class of accelerators which we believe will in the future implement plasma photocathodes, with possibly transformative impact on the research landscape. These are all-optical systems, where a laser-plasma-accelerator system replaces the linac.[6,29,30] LWFA intrinsically produces electron beams with high current and charge densities, which are primary requirements for driving a PWFA stage. In fact, LWFA and PWFA are highly complementary[6,31,32] such that a clear directionality of combining them in hybrid LWFA→PWFA setups is highly attractive. This idea holds for compact PWFA in general, but in particular for Trojan Horse systems, due to the inherent synchronization between electron beam driver and plasma photocathode injection laser pulse as both would emanate from the same laser system.[4,32] Linac-based PWFA, plasma photocathode R&D and hybrid LWFA→PWFA are all topics with a strong growth trajectory, and mutually are expected to reinforce and accelerate progress.[33] It is therefore anticipated that plasma photocathode-based ultralow emittance and unprecedented ultrabright 5D and 6D electron beams will be increasingly available for applications e.g. in the light source sector, even at university-scale laboratories. After seminal demonstration of experimental viability of the plasma photocathode process,[7] the next R&D phase is clearly centred on implementation of advanced plasma photocathodes to explore and realize the full electron emittance and brightness range, and to enhance stability. However, since the maximum brightness values which are currently suggested by theory are four orders of magnitude larger than even at the most advanced km-long hard x-ray facilities based on rf-linac technology, it is now increasingly important also to look forward and to analyse the next steps which will then be required to exploit such unprecedented emittance and brightness for light source applications.

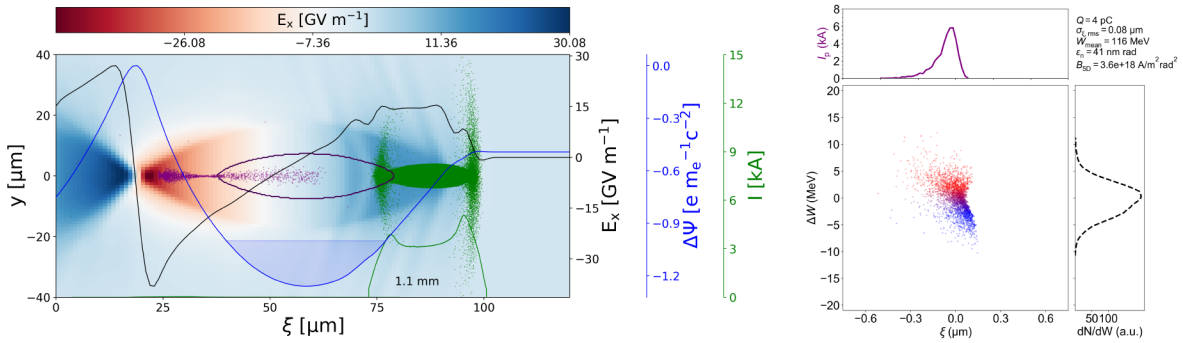

Figure 4. 3D PIC-simulation of a LCLS-II electron beam-driven Trojan Horse PWFA brightness booster stage. In the left panel, an LCLS-II-like (green dots) electron driver excites a nonlinear PWFA stage with a plasma photocathode laser injecting ultracold electrons (purple dots) within the trapping potential (purple solid ellipse). The blue line indicates the wake potential and the black line represents the corresponding longitudinal GV/m-scale accelerating gradient. In the right panel, the plasma photocathode injected witness beam longitudinal phase space with its current profile (purple solid line) and the spectral density (dashed black line) are shown. The witness beam has a peak current of $I_{\rm pk} \approx 6\,$kA with normalized emittance of $\epsilon_n \approx 41\,$nm resulting in ultrahigh 5D brightness $B_{\rm 5D} \approx 3.6 \times 10^{18}\,$A/mrad^2. This would constitute a 5D brightness boost by a factor of three to four orders of magnitude.

3. RADIATION SOURCES FROM ULTRAHIGH BRIGHTNESS ELECTRON BEAMS

X-ray and γ-ray radiation sources are fundamental research and diagnostic tools in chemistry, biology, physics and material science, and are also widely utilized in medicine and industry. Progress in generating such photon beams since the first observation of X-ray beams by Roentgen in 1895[34] has been tremendous, and starting from simple Bremsstrahlung-based incoherent X-ray tubes has seen the development of synchrotrons and then free-electron lasers for high power coherent radiation at sub-nanometer wavelengths. For even shorter wavelengths,

for example, Compton scattering processes are used to generate energetic γ-photon quanta. At the same time, the temporal pulse duration of such X-ray and γ-ray pulses are significantly decreased to typically tens of femtoseconds.[35,36] This scientific effort of producing shorter wavelength and duration radiation pulses is driven by many potential applications in fundamental science, medicine and industry .[37–39] For example, structural and physical state evolution in pump-probe experiments of materials and bio-samples may have a time span of tens of femtoseconds (10^{-15} s), and even more fundamental processes such as ionisation, isomerization, and ultrafast charge transfer in atoms, molecules, and nanostructures can occur on timescales down to the attoseconds (10^{-18} s) .[40–42] The underlying fundamental principle of radiation generation is based on utilizing electrons or electron beams of modest to ultrarelativistic energies in various ways to emit radiation at the desired wavelength. This has motivated the development of increasingly advanced dedicated electron injectors and accelerator structures based on rf technologies in order to produce the high quality electron beams required for high quality radiation production. For example, the path towards realizing the LCLS X-FEL required a fundamental improvement of the electron beam quality such as emittance obtainable from conventional accelerators by introducing novel photocathode technologies.

The plasma photocathode PWFA technology as discussed in Sec. 2 may allow a step change by producing electron beams with emittance and brightness many orders of magnitude better when compared to these high performance state-of-the-art accelerators. Such an improvement in particular in emittance and brightness therefore has huge potential, and e.g. may enable university laboratory-size hard X-ray free-electron lasers, high brightness γ-rays from Inverse-Compton Scattering, or X-ray Ion-Channel Lasers in compact m-scale setups and with inherent synchronization capabilities e.g. for pump-probe experiments. Such ultrahigh brightness electron beams may even enable to explore novel light source regimes not accessible by purely rf-cavity accelerator based technology. In the following sections, the impact of plasma photocathode-level brightness beams on FEL, ICS, and betatron/ICL type light sources will be discussed, and the specific challenges and prospects will be highlighted.

3.1 Trojan Horse PWFA Driven Hard X-ray FEL

The X-ray free-electron lasers are capable of producing fs-duration coherent radiation sources with very high power density, tunable in a wide range of the electromagnetic spectrum from extreme ultraviolet (XUV) to hard X-rays. FEL's enable novel research capabilities, for example the investigation of ultra-fast electronic and structural dynamics of ultra-small structures down to the atomic level. The FEL process is based on relativistic electron beams oscillating in an alternating magnetic field of an undulator. At the turning points of the resulting undulating trajectories, the electron beam emits spontaneous undulator radiation at the resonant wavelength:

$$\lambda_\mathrm{r} = \frac{\lambda_\mathrm{u}}{2\gamma^2}\left(1+\frac{K_\mathrm{u}^2}{2}\right), \tag{1}$$

where λ_u is the undulator period, γ is the Lorentz factor of the electron beam associated with its energy and $K_\mathrm{u} = 0.934\lambda_\mathrm{u}[\mathrm{cm}]B_0[T]$ is the undulator parameter with B_0 being the magnetic field amplitude.[35,43] The opening angle $\theta = K_\mathrm{u}/\gamma$ of the thus produced radiation depends upon the undulator parameter and the Lorentz factor of the electron beam. Thus, at highly relativistic energies when $\gamma \gg 1$ and $K_\mathrm{u} < 1$ the spontaneous synchrotron radiation becomes strongly forward-directed and collimated. This induces energy/density modulation within the electron beam at the resonance wavelength which in turn leads to more coherent emission. This positive feedback loop is initiating a collective instability resulting in microbunch formation.[35] The radiation power grows exponentially $P(z) \propto \exp(zL_\mathrm{g,1D}^{-1})$ along the undulator axis, where $L_\mathrm{g,1D} = \lambda_\mathrm{u}(4\pi\sqrt{3}\rho_\mathrm{FEL})^{-1}$ is the one dimensional gain length and ρ_FEL is the FEL Pierce parameter[35,43,44] which approximates the energy extraction efficiency and is typically of the order of $\rho_\mathrm{FEL} \sim 10^{-3} - 10^{-4}$ for hard X-ray FELs. This is the high gain FEL regime known as the Self Amplified Spontaneous Emission (SASE) FEL .[44] However, a hard X-ray FEL demands very high quality electron beams. In order to drive a hard X-ray FEL the following key thresholds and criteria have to be fulfilled:

- Emittance criterion ("Pellegrini criterion"):[35,44] $\epsilon_\mathrm{n} \lesssim \gamma\lambda_\mathrm{r}/4\pi$. The normalized emittance of the electron beam has to be low in order to achieve lasing at the resonant wavelength λ_r at a given electron beam

Lorentz factor γ. Because in rf-based linacs typical obtainable emittances are at the $\epsilon_n \sim 1\,\mu$m rad-level, this requires multi-GeV electron energies to satisfy this condition.

- Energy spread criterion (Pierce parameter):[44] The relative energy spread of the electron beam has to be strictly smaller than the FEL Pierce parameter $\Delta W_{rms}/W_{mean} < \rho_{FEL}$. In conventional rf-based accelerators this is also facilitated by accelerating the electron beam to multi-GeV energies in km-size linacs.

- Compactness of the X-FEL:[1,6,45] The gain length $L_{g,1D}$ scales favourably with the electron beam brightness $L_{g,1D} \propto B_{6D}^{-1/3}$ such that ultrastrong gain, and ultrashort FEL gain lengths can be realized by improving the electron beam brightness.

In the past decades, significant effort has been invested to improve the output energy characteristics of plasma-based accelerators and to get close to reaching FEL gain.[46,47] First steps have been reached by showing spontaneous undulator radiation in the visible[46] and soft X-ray range[48] from electron beams produced via LWFA, but the threshold of realizing FEL gain, let alone gain in an X-FEL, remains very challenging. This is because of the above discussed minimum demands on the electron beam quality for an FEL, and the optimum parameter reach of conventional LWFA-based electron beams, which hardly overlap. In addition to the need to improve key characteristics such as energy spread and emittance of plasma accelerator output substantially to overcome the key thresholds required for X-FEL by a sufficient margin, precise control over the electron beam parameters such as energy, energy spread, emittance, current and pointing is required to maintain stable X-FEL performance on a shot-to-shot basis. For example, variation of electron beam energy $\Delta\gamma$ will result in strong variation of the resonance wavelength because of the $\lambda_r \propto \gamma^{-2}$-scaling which in turn can change the FEL operation parameter regime from shot-to-shot. The positioning and pointing jitter of the electron beam may cause a spread in the undulator parameter ΔK_u which will alter the resonance wavelength $\lambda_r \propto (1 + K_u^2/2)$ as well. These very basic considerations clearly emphasize the need and importance of ultrahigh quality and stable electron beams for FEL/X-FEL applications.

The Trojan Horse PWFA method and its further enhancement by the escort bunch dechirping approach are developed to overcome these thresholds and challenges amply, and in a controlled and flexible fashion (see Sec. 2.1). With regard to emittance, nm-rad normalized emittance levels enabled by the plasma photocathode allow to satisfy the Pellegrini criterion already at few GeV energies even for hard X-ray wavelengths and at the same time, the relative energy spread reach of the witness beam extends to as low as 0.01 % or even lower. Such low energy spread is clearly sufficient to beat the FEL energy spread criterion, but also facilitates electron beam extraction from the plasma stage and its transport in electron beam optics transport lines towards the undulator without quality degradation. Finally, due to the ultrahigh 6D brightness of these electron beams, the FEL gain length is expected to be very short, enabling saturation in university and industry scale laboratories, and substantially reducing the spatial footprint and costs of such systems. The stability aspect can be resolved by operating at longer plasma wavelengths ($100 - 500\,\mu$m) because then the synchronisation and alignment stability requirements of plasma photocathode injection are significantly reduced.[7,10] These considerations motivated a dedicated beginning R&D programme on "PWFA-FEL" funded by the UK Science and Technology Facilities Council (STFC) which will explore the generation of ultrahigh (5D and 6D) brightness beams via plasma photocathodes, extraction, transport and utilization for advanced X-FEL operation, including ultimately aiming at sub-femtosecond ultrabright X-ray pulses, which may allow for the first time to observe electronic motion inside matter on natural timescales. From a viewpoint more focused on high energy physics, such a compact plasma-based accelerator driven X-FEL can be considered as an extremely high impact milestone towards a potential future plasma-based linear collider. These two major community goals therefore constructively mutually reinforce each other,[49] since they share major goals such as ultralow emittance and controllability.

3.2 Inverse Compton Scattering

Another method for generation of X- or γ-ray pulses from relativistic electron beams substitutes the typically permanent magnetic field based undulators in FELs by the counterpropagating electromagnetic field of an intense laser pulse. This configuration is known as inverse Compton scattering. It allows for considerable energy transfer because the laser oscillation period is orders of magnitude smaller compared to to the magnetic alternative.[50]

The strong scaling resulting from this substitution substantially boosts the energy E_L of incident laser photons given by the well-known relation $\frac{E_\gamma}{E_\mathrm{L}} = \frac{4\gamma^2}{1+\gamma^2\theta^2}$. Here, γ denotes the electron Lorentz factor, and θ represents the scattering angle within a cone opening with $\sim 1/\gamma$ centered on the electron beam axis. Thus, comparably low-energetic electrons of the order of several hundred MeV already suffice for generation of directed MeV-class photons within a pulse length given by the electron beam duration.These properties particularly emphasize the application of plasma electron accelerators for ICS sources, as they routinely reach these energies in very compact setups, and inherently produce ultra-short electron beams.

Capabilities of X-ray pulses for controlled excitation and characterization of nuclear processes such as nuclear resonance fluorescence depend on their absolute and relative bandwidth.[51,52] This quantity is determined by the phase space properties of electron beam and laser pulse. Combining the latter, namely natural bandwidth, pulse diffraction and intensity dependencies ,[53] yields a single term $\frac{\Delta\sigma_L}{\sigma_L}^2$ considered constant, small and linear in this context. Then, the relative radiation bandwidth can be approximated by [52]

$$\left(\frac{\Delta E_\gamma}{E_\gamma}\right)^2 \approx \left(2\frac{\Delta\gamma}{\gamma}\right)^2 + \left(\frac{\gamma^2\sigma_\theta^2}{4}\right)^2 + \left(\frac{\Delta\sigma_L}{\sigma_L}\right)^2. \tag{2}$$

Monochromatic X-ray pulses therefore generally demand for low electron beam energy spread, as it defines the minimal bandwidth obtainable in any interaction regime. Elevated electron energies, furthermore, couple substantially with the beam's divergence σ_θ and cause spectral broadening for typical electron beams from plasma accelerators. Summarizing, these considerations express the considerable influence of electron beam 6D brightness on the scattered photon pulse brilliance. Beams generated by a plasma photocathode wakefield accelerator fortunately inherit the short duration and suitable energies typical for plasma accelerators accompanied by its unique features of low energy spread[10] and ultra-low emittance.[45] Particularly the latter guarantees small beam divergence associated to narrow bandwidth in the range of 1-10% even at high beam energies as displayed in Fig. 5. ICS sources based on plasma photocathode-generated beams therefore offer outstanding prospects among other plasma-based ICS approaches and may provide complementary γ-rays with high brilliance per shot without spectral filtering. Similar to other plasma-based ICS sources, technological progress allowing highly increased repetition rates are necessary for generating the average flux already produced in conventional facilities. The high flexibility unique to the plasma photocathode combined with its confined ionisation and trapping volumes offers controlled injection of multiple high-quality beams. Due to the trapping dynamics associated to ionization injection in non-linear plasma waves ,[54] these beams can be trapped spatially separated if electrons are released at different longitudinal positions. Additionally tuning the corresponding lab-frame injection position generates beams at different times, which facilitates arbitrary spectral separation. In an ICS scattering event, this witness beam pair generates well-defined, clearly separated and inherently synchronized multi-color radiation pulses.

3.3 From Betatron Radiation to Ion Channel Laser

The plasma itself can also provide the undulating forces which can be exploited for light source production and diagnostics, since the immobile ion background provides a linear restoring force pointing transversely towards the propagation axis inside the plasma cavity. This serves as an inherent focusing channel which keeps injected and accelerating electron bunches transversely compressed, but can also manifest in a plasma wiggler/undulator if an electron beam is injected off-axis into the plasma cavity or if it is otherwise kicked transversely. Such an electron beam will then start wiggling around the propagation axis and thereby emits incoherent synchrotron-like radiation known as plasma betatron radiation.[42,56,57] In the collinear (or countercollinear) Trojan Horse scheme, injected electrons are typically released on-axis in order to minimize the injected electron beam emittance (see Fig. 6 (left)), while misalignment of the plasma photocathode laser pulse with respect to the driver beam consequently realizes off-axis injection, as demonstrated in the 3D PIC simulation in Fig. 6 (right) and as shown in Ref. 45. The electrons born by the plasma photocathode off-axis are immediately attracted back to the propagation axis by the linear restoring force of the plasma cavity, and are accelerated in the forward direction. While the initial residual transverse momentum of the plasma photocathode process itself is negligible, the transverse momentum from the restoring force of the plasma channel makes the electrons overshoot the axis transversely, and they then continue oscillating in the transverse electric fields at their trapping position inside

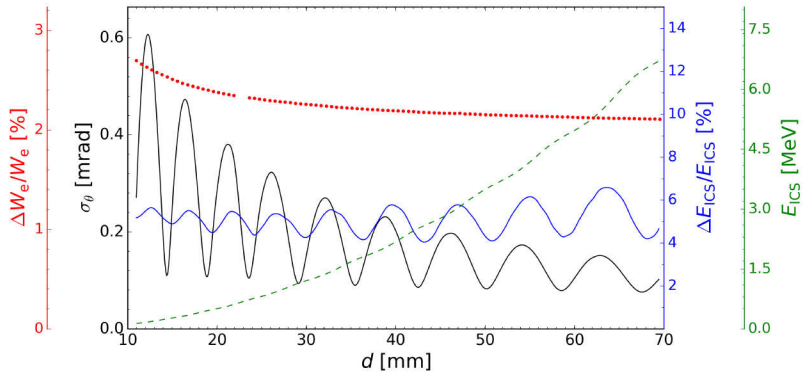

Figure 5. Evolution of electron beam and momentary ICS pulse parameters along a plasma photocathode wakefield accelerator. Here, the plasma wavelength $\lambda_p \approx 300\,\mu$m. The beam's energy spread (red) saturates at $\sim 2.2\,\%$ (r.m.s) because of self-beam loading. The energy spread compensation technique [10] is not applied here. Due to the combined effect of weak focusing forces and ultra-low emittance ~ 30 nm rad, the beam's r.m.s. divergence (black) reaches the level of $\sigma_\theta \approx 0.1$ mrad. The simulated [55] green and blue curves outline the momentary ICS energy and r.m.s. bandwidth, respectively. The influence of laser parameters on the bandwidth is negligible compared to each term governed by the electron beam. Even though MeV-level x-rays are generated, the corresponding bandwidth remains well below $10\,\%$. This is caused by the low divergence, which suppresses strong broadening and limits the ICS bandwidth to the energy spread term in 2. Thus, reduction of energy spread could substantially narrow the spectral ICS distribution.

the blowout at the betatron frequency $\omega_\beta \simeq \omega_\mathrm{p}/\sqrt{2\gamma}$, where $\omega_\mathrm{p} = 2\pi c/\lambda_\mathrm{p}$ is the plasma frequency. By tuning the off-axis release position and the longitudinal release/trapping position, therefore the betatron amplitude can be fine-tuned. Another benefit arising from the decoupled nature of this injection scheme particularly in context of betatron radiation and ion-channel laser is flexible control over the betatron radiation polarization in a convenient manner. For example, an offset of the release laser pulse only in one transverse direction leads to planar oscillation of the electron beam in this plane, resulting in linearly polarized radiation, whereas releasing electrons with an offset in both transverse dimensions will result in bi-planar oscillation, allowing to generate tunable circularly polarized radiation. Since plasma photocathode injection works with almost arbitrary plasma blowout sizes, a wide range of betatron amplitudes and modalities thus can be accessed. The betatron frequency of the electron beam will increase quickly with the energy gain of the electron beam because of the $\omega_\beta \propto \gamma^{-1/2}$-scaling. Neglecting the acceleration in the plasma cavity allows defining, in practical units, the electron oscillation period $\lambda_{\mathrm{u},\beta}[\mu\mathrm{m}] = 4.72 \times 10^{10}\sqrt{\gamma/n_0[\mathrm{cm}^{-3}]}$ and strength parameter $K_{\mathrm{u},\beta} = 1.33 \times 10^{-10}\sqrt{\gamma/n_0[\mathrm{cm}^{-3}]}r_\beta[\mu\mathrm{m}]$, where $r_\beta = \sqrt{x_\beta^2 + y_\beta^2}$ is the radial betatron amplitude .[42] For a typical plasma density of $n_0 = 10^{17}\,\mathrm{cm}^{-3}$ and beam energy of $\gamma = 2000$ this results in an oscillation period of $\lambda_{\mathrm{u},\beta} = 6.7\,\mathrm{mm}$, which is significantly shorter than in typical magnetic undulators. The spectral properties of the betatron radiation are similar to incoherent synchrotron radiation because the radiation wavelength is changing with the acceleration of the electron beam and prevents coherent overlap. Thus, collective effects such as in FEL's can only take place if the witness beam energy and the betatron period remain constant over a sufficient propagation distance. Such a situation can be created in the ion-channel laser regime, originally proposed in Ref. 58 as a plasma-based compact alternative to magnetic undulator based FELs.

The ICL scenario requires that the electrons inside the plasma undulator experience a strong transverse focusing force, but are not affected by longitudinal wakefields.[42] These conditions can be found in a transversely confined plasma filament purely consisting of ions. There, a linear restoring force is provided by the ion column, while no plasma electrons are around to develop an accelerating wakefield. Such a wakeless ion channel can be generated in a PWFA-like configuration, where a high peak-current electron beam drives a blowout in a thin, pre-formed plasma channel. If the plasma channel is considerably narrower than the nominal blowout radius, the drive beam expels the plasma electrons beyond the initial ion column such that the transverse kinetic energy of these plasma electrons exceeds the restoring electric potential energy of the remaining ions. Consequently, the plasma electrons are simply "snowploughed" away and the wakefield collapses. Another variation to achieve

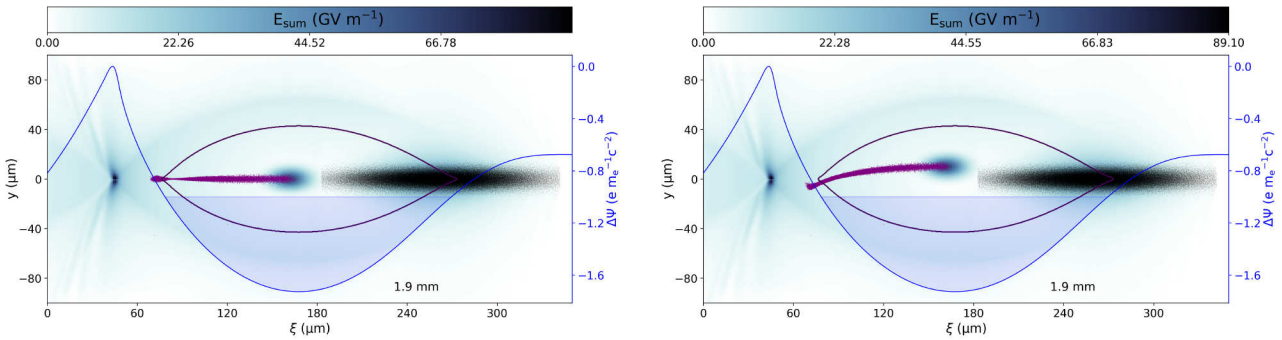

Figure 6. A FACET-II electron beam-driven Trojan Horse PWFA stage in a wide plasma channel modelled with the 3D PIC code Vsim.[13] Right panel: a FACET-II electron beam (black dots) excites a nonlinear PWFA-stage of plasma density $n_0 \approx 1.8 \times 10^{16}\,\mathrm{cm}^{-3}$ corresponding to a plasma wavelength of $\lambda_\mathrm{p} \approx 250\,\mu$m. A co-propagation plasma photocathode laser pulse releases helium electrons (purple dots) on-axis within the trapping potential boundary (purple ellipse), the corresponding on-axis wake potential (solid blue line) satisfies the trapping condition $\Delta\Psi < -1$ as well. At the release position of the helium electrons, at the potential minimum, the geometric sum of the wakefield E_sum (blue colormap) is zero. This reduces the transverse kick from the wakefield on the freshly born electrons. The plasma cavity is significantly large than in a $\lambda_\mathrm{p} \approx 250\,\mu$m-case which relaxes the synchronisation requirements on the injection laser pulse. Right panel: The plasma photocathode laser pulse is purposefully misaligned with respect to the driver beam. Now, the helium electrons are liberated off-axis which leads to excitation of betatron oscillation in controlled and flexible fashion. For example, arbitrary degree of misalignment of the the injection laser pulse may allow to control the polarization of the resulting betatron and ICL radiation.

constant wiggling could be a plasma density downramp, tuned such that the witness electron beam is then longitudinally placed in the centre of the then larger plasma cavity, where no accelerating/decelerating fields are present, without changing its distance to the driver electron beam.

It is particularly attractive to realize an ICL in conjunction with a PWFA delivering high-brightness witness beams. In this scenario, a pre-formed plasma channel consisting of two distinct sections with different plasma channel widths are employed to switch from PWFA to ICL mode at a given target electron energy. Initially, during injection and the PWFA stage, the plasma channel should be sufficiently wide to accommodate a stable blowout to generate and accelerate the witness beam. As soon as the witness beam reaches the desired energy, the plasma channel width is rapidly reduced in the ICL section. The driver beam consequently then removes all plasma electrons from the channel and the wakefield vanishes. A slight transverse offset of the witness beam with respect to the remaining ion column induces persistent harmonic oscillations, thus triggering the ICL process. A suitable experimental scenario to generate such a plasma environment is synergistic with the strongly preferable laser-based plasma preionization as a central building block of Trojan Horse PWFA. While in E-210 as described above and in Ref. 7, and as shown in Fig. 3, left panel, the plasma channel did not have uniform width but assumes a shape dictated by the specifics of the axicon/axilens-based preionization laser intensity profile. In fact, in E-210, the preionized plasma channel width was an experimental bottleneck where we observed transitions from the witness beam being in the accelerating phase of the plasma wave to being in the centre of the plasma wave during transverse narrowing of the channel, where no acceleration or deceleration occurs, to being in the decelerating phase of the plasma wave, consistent with the considerations above. As indicated in Ref. 10, supplementary figure 3, one could practically generate a controlled version of such a dual-section plasma e.g. by a counterpropagating preionization laser pulse to generate the thin wakeless plasma channel for ICL, while the wider PWFA plasma section would be generated by a co-propagating preionization laser pulse as in E-210. By shifting the counterpropagating preionization laser transversally and/or by introducing an oblique plasma density boundary and/or by kicking the electron beam transversally for example by an external magnetic field or by a plasma torch filament, an arbitrary transverse (additional) oscillation amplitude can be set up.

In contrast to FELs, the required ICL Pierce parameter may be on the order of $\rho_\mathrm{ICL} \sim 10^{-2}$,[59] which significantly relaxes the requirements on the electron beam energy spread.[42,60] Still, to access coherent amplification of soft or hard X-ray betatron radiation, a normalized witness beam emittance on the order of nm-rad is required,[58]

which currently is beyond the reach of conventional as well as plasma-based accelerators. However, the plasma photocathode allows achieving the demanding emittance requirements as discussed above, as well as the energy spread requirement. The experimental feasibility of such an ICL can also potentially be explored in upcoming experiments at the FACET-II facility.

4. SUMMARY AND OUTLOOK

Beam-driven plasma wakefield accelerators have passed the proof-of-concept phase and are evolving into mature technology supporting accelerating gradients three to four orders of magnitude higher than rf-based conventional accelerators. The GV/m-scale electric fields inside the wakefield allow, consequently, acceleration of charged particles to multi-GeV energies in metre-scale acceleration distances compared with kilometer-size state-of-the-art technologies. This capability combined with the plasma photocathode [45] injection mechanism enables not only to facilitate ultrahigh accelerating gradients but at the same time paves the way to produce 'designer' electron beams of ultrahigh 5D brightness. Further development of the plasma photocathode mechanism with the escort beam energy chirp compensation method [10] may support production of electron beams with unprecedented 6D-brightness with relative energy spread values down to the 0.01 %-level already at few GeV electron energies in a single acceleration stage.

The SLAC FACET E-210: Trojan Horse PWFA experiment has demonstrated two distinct injection methodes in PWFA for the first time, namely the plasma photocathode 'Trojan Horse' injection in 90°-geometry and all-optical 'Plasma Torch' downramp injection.[7] These proof-of-concept experiments are encouraging pioneering milestones on the way towards generation of plasma-based ultrahigh brightness electron beams. Research on this will be driven forward further, at SLAC emerging from E-210 at FACET into an expanded programme at FACET-II in the E-310–317 experiments towards highest quality electron beam production via the plasma photocathode injection PWFA scheme, but also will include research on novel plasma-based diagnostics. The underlying idea here is that while plasma-based wakefield acceleration can sustain orders of magnitude larger accelerating fields than state-of-the-art, and is aiming for production of electron beams orders of magnitude larger than state-of-the-art, also requires diagnostics which are orders of magnitude more sensitive than state-of-the-art. For example, there is currently no method known which would allow measurement of nm-scale emittance kA-level current beams or their associated brightness. The formation of plasma via exponentially sensitive tunneling ionization, and its collective response to such beams, could be a pathway to measure important parameters of these extreme beams, analogical in nature to how collective motion of plasma electrons and tunneling ionization based plasma photocathodes enable to produce such extreme beams which exceed damage thresholds of normal matter in the first place.

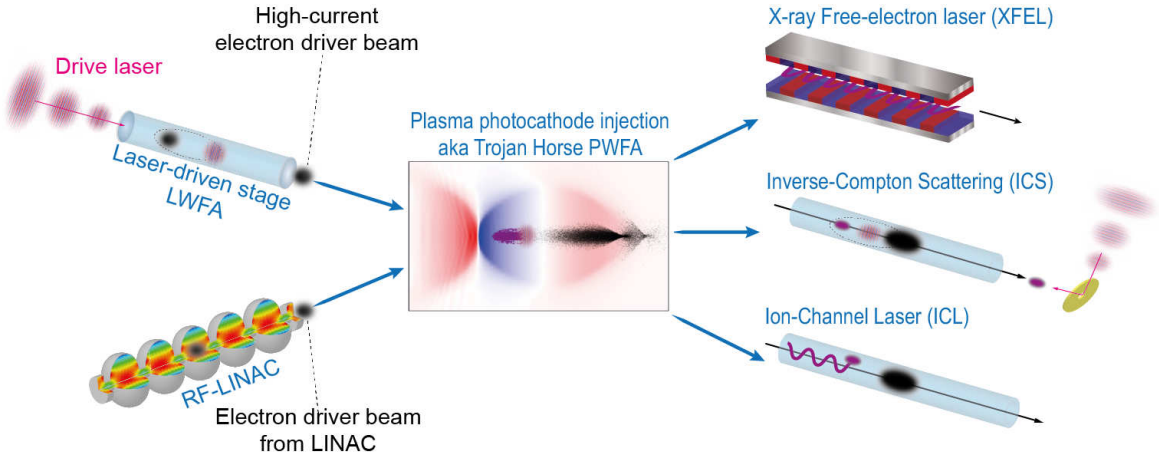

Figure 7. Conceptual overview of the Trojan Horse PWFA acting as gateway to boost brightness of linac-generated and LWFA-produced electron beams for key light source applications such as X-FEL, ICL, and ICS.

At the same time, R&D will also be expanded to further linac-based PWFA-capable facilities, and to hybrid LWFA→PWFA approaches .[29,30] This will accelerate the development and prototyping of plasma photocathode electron guns as standardized ultrahigh brightness electron beam source technology, and will allow harnessing of the impact which is expected from ultrabright electron beams for applications such as light sources. Figure 7 provides a schematic overview on the plasma photocathode PWFA method as brightness transformer stage for electron beams from LWFA as well as from conventional linacs, in order to unlock realization of transformative light source applications such as X-FEL, ICS, and ICL on university- and industry-laboratory scale.

ACKNOWLEDGMENTS

The FACET E210: Trojan Horse plasma wakefield acceleration experiment was built and operated with support from UCLA (US DOE contract DE-SC0009914), RadiaBeam Technologies (DOE contract DE-SC0009533), the FACET E200 team and the U.S. Department of Energy under contract number DE-AC02-76SF00515, H2020 EuPRAXIA (Grant No. 653782), EPSRC (Grant No. EP/N028694/1). This work used computational resources of the National Energy Research Scientific Computing Center, which is supported by DOE DE-AC02-05CH11231, of JURECA (Project hhh36), of HLRN and of Shaheen (Project k1191). The US DOE Office of High Energy Physics under Award No. DE-SC0013855.

REFERENCES

[1] S. Di Mitri, "On the importance of electron beam brightness in high gain free electron lasers," *Photonics* **2**(2), pp. 317–341, 2015.

[2] I. Blumenfeld *et al.*, "Energy doubling of 42 gev electrons in a metre-scale plasma wakefield accelerator," *Nature* **445**(7129), pp. 741–744, 2007.

[3] M. Litos *et al.*, "High-efficiency acceleration of an electron beam in a plasma wakefield accelerator," *Nature* **515**(7525), pp. 92–95, 2014.

[4] B. Hidding, G. Pretzler, J. B. Rosenzweig, T. Königstein, D. Schiller, and D. L. Bruhwiler, "Ultracold electron bunch generation via plasma photocathode emission and acceleration in a beam-driven plasma blowout," *Phys. Rev. Lett.* **108**, p. 035001, Jan 2012.

[5] B. Hidding, T. Koenigstein, S. Karsch, O. Willi, G. Pretzler, and J. B. Rosenzweig, "Hybrid laserplasma wakefield acceleration," *AIP Conference Proceedings* **1299**(1), pp. 483–488, 2010.

[6] B. Hidding, G. G. Manahan, O. Karger, A. Knetsch, G. Wittig, D. A. Jaroszynski, Z.-M. Sheng, Y. Xi, A. Deng, J. B. Rosenzweig, G. Andonian, A. Murokh, G. Pretzler, D. L. Bruhwiler, and J. Smith, "Ultrahigh brightness bunches from hybrid plasma accelerators as drivers of 5th generation light sources," *Journal of Physics B: Atomic, Molecular and Optical Physics* **47**(23), p. 234010, 2014.

[7] A. Deng, O. S. Karger, T. Heinemann, A. Knetsch, P. Scherkl, G. G. Manahan, A. Beaton, D. Ullmann, G. Wittig, A. F. Habib, Y. Xi, M. D. Litos, B. D. OShea, S. Gessner, C. I. Clarke, S. Z. Green, C. A. Lindstrom, E. Adli, R. Zgadzaj, M. C. Downer, G. Andonian, A. Murokh, D. L. Bruhwiler, J. R. Cary, M. J. Hogan, V. Yakimenko, J. B. Rosenzweig, and B. Hidding, "Generation and acceleration of electron bunches from a plasma photocathode," *Nature Physics* , August 2019.

[8] P. Antici, A. Bacci, C. Benedetti, E. Chiadroni, M. Ferrario, A. R. Rossi, L. Lancia, M. Migliorati, A. Mostacci, L. Palumbo, and L. Serafini, "Laser-driven electron beamlines generated by coupling laser-plasma sources with conventional transport systems," *Journal of Applied Physics* **112**(4), p. 044902, 2012.

[9] T. Mehrling, J. Grebenyuk, F. S. Tsung, K. Floettmann, and J. Osterhoff, "Transverse emittance growth in staged laser-wakefield acceleration," *Phys. Rev. ST Accel. Beams* **15**, p. 111303, Nov 2012.

[10] G. Manahan, A. Habib, P. Scherkl, P. Delinikolas, A. Beaton, A. Knetsch, O. Karger, G. Wittig, T. Heinemann, Z. Sheng, J. Cary, D. Bruhwiler, J. Rosenzweig, and B. Hidding, "Single-stage plasma-based correlated energy spread compensation for ultrahigh 6d brightness electron beams," *Nature Communications* **8**, June 2017.

[11] T. Katsouleas, S. Wilks, P. Chen, J. Dawson, and J. Su, "Beam loading in plasma accelerators," *Particle Accelerators* **22**, pp. 81–99, 1987.

[12] M. Tzoufras, W. Lu, F. S. Tsung, C. Huang, W. B. Mori, T. Katsouleas, J. Vieira, R. A. Fonseca, and L. O. Silva, "Beam loading in the nonlinear regime of plasma-based acceleration," *Phys. Rev. Lett.* **101**, p. 145002, Sep 2008.

[13] C. Nieter and J. R. Cary, "Vorpal: a versatile plasma simulation code," *Journal of Computational Physics* **196**(2), pp. 448 – 473, 2004.

[14] V. Yakimenko, N. Lipkowitz, C. Clarke, M. Hogan, G. Yocky, C. Hast, S. Green, Y. Cai, N. Phinney, and G. White, "Facet-ii accelerator research with beams of extreme intensities," 2016.

[15] N. Barov, J. B. Rosenzweig, M. C. Thompson, and R. B. Yoder, "Energy loss of a high-charge bunched electron beam in plasma: Analysis," *Phys. Rev. ST Accel. Beams* **7**, p. 061301, Jun 2004.

[16] G. G. Manahan, A. Deng, O. Karger, Y. Xi, A. Knetsch, M. Litos, G. Wittig, T. Heinemann, J. Smith, Z. M. Sheng, D. A. Jaroszynski, G. Andonian, D. L. Bruhwiler, J. B. Rosenzweig, and B. Hidding, "Hot spots and dark current in advanced plasma wakefield accelerators," *Phys. Rev. Accel. Beams* **19**, p. 011303, Jan 2016.

[17] K. Moon, S. Kumar, M. Hur, and M. Chung, "Longitudinal phase space dynamics of witness bunch during the trojan horse injection for plasma-based particle accelerators," *Physics of Plasmas* **26**(7), p. 073103, 2019.

[18] G. G. Manahan, A. F. Habib, P. Scherkl, D. Ullmann, A. Beaton, A. Sutherland, G. Kirwan, P. Delinikolas, T. Heinemann, R. Altuijri, A. Knetsch, O. Karger, N. M. Cook, D. L. Bruhwiler, Z.-M. Sheng, J. B. Rosenzweig, and B. Hidding, "Advanced schemes for underdense plasma photocathode wakefield accelerators: pathways towards ultrahigh brightness electron beams," *Philosophical Transactions of the Royal Society A: Mathematical, Physical and Engineering Sciences* **377**(2151), p. 20180182, 2019.

[19] B. Hidding *et al.*, "Tunable electron multibunch production in plasma wakefield accelerators," *arXiv* , p. 1403.1109, 2014.

[20] Y. P. Wu, J. F. Hua, Z. Zhou, J. Zhang, S. Liu, B. Peng, Y. Fang, Z. Nie, X. N. Ning, C.-H. Pai, Y. C. Du, W. Lu, C. J. Zhang, W. B. Mori, and C. Joshi, "Phase space dynamics of a plasma wakefield dechirper for energy spread reduction," *Phys. Rev. Lett.* **122**, p. 204804, May 2019.

[21] R. D'Arcy, S. Wesch, A. Aschikhin, S. Bohlen, C. Behrens, M. J. Garland, L. Goldberg, P. Gonzalez, A. Knetsch, V. Libov, A. M. de la Ossa, M. Meisel, T. J. Mehrling, P. Niknejadi, K. Poder, J.-H. Röckemann, L. Schaper, B. Schmidt, S. Schröder, C. Palmer, J.-P. Schwinkendorf, B. Sheeran, M. J. V. Streeter, G. Tauscher, V. Wacker, and J. Osterhoff, "Tunable plasma-based energy dechirper," *Phys. Rev. Lett.* **122**, p. 034801, Jan 2019.

[22] V. Shpakov, M. P. Anania, M. Bellaveglia, A. Biagioni, F. Bisesto, F. Cardelli, M. Cesarini, E. Chiadroni, A. Cianchi, G. Costa, M. Croia, A. Del Dotto, D. Di Giovenale, M. Diomede, M. Ferrario, F. Filippi, A. Giribono, V. Lollo, M. Marongiu, V. Martinelli, A. Mostacci, L. Piersanti, G. Di Pirro, R. Pompili, S. Romeo, J. Scifo, C. Vaccarezza, F. Villa, and A. Zigler, "Longitudinal phase-space manipulation with beam-driven plasma wakefields," *Phys. Rev. Lett.* **122**, p. 114801, Mar 2019.

[23] S. Corde, E. Adli, J. M. Allen, W. An, C. I. Clarke, C. E. Clayton, J. P. Delahaye, J. Frederico, S. Gessner, S. Z. Green, M. J. Hogan, C. Joshi, N. Lipkowitz, M. Litos, W. Lu, K. A. Marsh, W. B. Mori, M. Schmeltz, N. Vafaei-Najafabadi, D. Walz, V. Yakimenko, and G. Yocky, "Multi-gigaelectronvolt acceleration of positrons in a self-loaded plasma wakefield," *Nature* **524**, pp. 442 EP –, Aug 2015.

[24] S. Gessner, E. Adli, J. M. Allen, W. An, C. I. Clarke, C. E. Clayton, S. Corde, J. Delahaye, J. Frederico, S. Z. Green, *et al.*, "Demonstration of a positron beam-driven hollow channel plasma wakefield accelerator," *Nature communications* **7**, p. 11785, 2016.

[25] B. Hidding *et al.*, "First measurements of trojan horse injection in a plasma wakefield accelerator," p. TUYB1, 2017.

[26] G. Wittig, O. Karger, A. Knetsch, Y. Xi, A. Deng, J. B. Rosenzweig, D. L. Bruhwiler, J. Smith, G. G. Manahan, Z.-M. Sheng, D. A. Jaroszynski, and B. Hidding, "Optical plasma torch electron bunch generation in plasma wakefield accelerators," *Phys. Rev. ST Accel. Beams* **18**, p. 081304, Aug 2015.

[27] G. Wittig, O. S. Karger, A. Knetsch, Y. Xi, A. Deng, J. B. Rosenzweig, D. L. Bruhwiler, J. Smith, Z.-M. Sheng, D. A. Jaroszynski, G. G. Manahan, and B. Hidding, "Electron beam manipulation, injection and acceleration in plasma wakefield accelerators by optically generated plasma density spikes," *Nuclear Instruments and Methods in Physics Research Section A: Accelerators, Spectrometers, Detectors and Associated Equipment* **829**, pp. 83 – 87, 2016. 2nd European Advanced Accelerator Concepts Workshop - EAAC 2015.

[28] A. Knetsch *et al.*, "Downramp-assisted underdense photocathode electron bunch generation in plasma wakefield accelerators," *arXiv* , p. 1412.4844, 2014.

[29] B. Hidding, T. Koenigstein, J. Osterholz, S. Karsch, O. Willi, and G. Pretzler, "Monoenergetic energy doubling in a hybrid laser-plasma wakefield accelerator," *Phys. Rev. Lett.* **104**, p. 195002, May 2010.

[30] M. F. Gilljohann, H. Ding, A. Döpp, J. Götzfried, S. Schindler, G. Schilling, S. Corde, A. Debus, T. Heinemann, B. Hidding, S. M. Hooker, A. Irman, O. Kononenko, T. Kurz, A. Martinez de la Ossa, U. Schramm, and S. Karsch, "Direct observation of plasma waves and dynamics induced by laser-accelerated electron beams," *Phys. Rev. X* **9**, p. 011046, Mar 2019.

[31] A. M. de la Ossa, R. W. Assmann, M. Bussmann, S. Corde, J. P. C. Cabada, A. Debus, A. Dpp, A. F. Pousa, M. F. Gilljohann, T. Heinemann, B. Hidding, A. Irman, S. Karsch, O. Kononenko, T. Kurz, J. Osterhoff, R. Pausch, S. Schbel, and U. Schramm, "Hybrid lwfa–pwfa staging as a beam energy and brightness transformer: conceptual design and simulations," *Philosophical Transactions of the Royal Society A: Mathematical, Physical and Engineering Sciences* **377**(2151), p. 20180175, 2019.

[32] B. Hidding, A. Beaton, L. Boulton, S. Corde, A. Doepp, F. A. Habib, T. Heinemann, A. Irman, S. Karsch, G. Kirwan, A. Knetsch, G. G. Manahan, A. Martinez de la Ossa, A. Nutter, P. Scherkl, U. Schramm, and D. Ullmann, "Fundamentals and applications of hybrid lwfa-pwfa," *Applied Sciences* **9**(13), 2019.

[33] B. Hidding, B. Foster, M. J. Hogan, P. Muggli, and J. B. Rosenzweig, "Directions in plasma wakefield acceleration," *Philosophical Transactions of the Royal Society A: Mathematical, Physical and Engineering Sciences* **377**(2151), p. 20190215, 2019.

[34] W. C. Röntgen, "Aus den sitzungsberichten der würzburger physik.-medic," *Würzburg: Gesellschaft* , pp. 137–147, 1895.

[35] C. Pellegrini, "The history of x-ray free-electron lasers," *The European Physical Journal H* **37**, pp. 659–708, Oct 2012.

[36] P. G. O'shea and H. P. Freund, "Free-electron lasers: Status and applications," *Science* **292**(5523), pp. 1853–1858, 2001.

[37] A. Zewail, R. Marcus, J. Manz, V. Sundström, T. Pullerits, R. van Grondelle, J. Jortner, M. Bixon, M. Karplus, W. Lineberger, *et al.*, "Femtochemistry and femtobiology: Ultrafast reaction dynamics at atomic-scale resolution," in *Nobel Symposium*, **101**, 1996.

[38] I. Nenner, H. Dexpert, and M. Bessiere, "Synchrotron radiation and applications," in *Chemical analysis and characterization*, 1989.

[39] A. L. Robinson, "History of synchrotron radiation," *Synchrotron Radiation News* **28**(4), pp. 4–9, 2015.

[40] R. Neutze, R. Wouts, D. van der Spoel, E. Weckert, and J. Hajdu, "Potential for biomolecular imaging with femtosecond x-ray pulses," *Nature* **406**(6797), pp. 752–757, 2000.

[41] H. N. Chapman, P. Fromme, A. Barty, T. A. White, R. A. Kirian, A. Aquila, M. S. Hunter, J. Schulz, D. P. DePonte, U. Weierstall, *et al.*, "Femtosecond x-ray protein nanocrystallography," *Nature* **470**(7332), pp. 73–77, 2011.

[42] S. Corde, K. T. Phuoc, G. Lambert, R. Fitour, V. Malka, A. Rousse, A. Beck, and E. Lefebvre, "Femtosecond x rays from laser-plasma accelerators," *Reviews of Modern Physics* **85**(1), p. 1, 2013.

[43] B. W. McNeil and N. R. Thompson, "X-ray free-electron lasers," *Nature photonics* **4**(12), p. 814, 2010.

[44] R. Bonifacio, C. Pellegrini, and L. Narducci, "Collective instabilities and high gain regime in a free electron laser," *Opt. Commun.* **50**, pp. 373–378, 1984.

[45] B. Hidding, G. Pretzler, J. B. Rosenzweig, T. Königstein, D. Schiller, and D. L. Bruhwiler, "Ultracold electron bunch generation via plasma photocathode emission and acceleration in a beam-driven plasma blowout," *Phys. Rev. Lett.* **108**, p. 035001, Jan 2012.

[46] H.-P. Schlenvoigt, K. Haupt, A. Debus, F. Budde, O. Jackel, S. Pfotenhauer, H. Schwoerer, E. Rohwer, J. G. Gallacher, E. Brunetti, R. P. Shanks, S. M. Wiggins, and D. A. Jaroszynski, "A compact synchrotron radiation source driven by a laser-plasma wakefield accelerator," *Nat Phys* **4**(2), pp. 130–133, 2008.

[47] Z. Huang, Y. Ding, and C. B. Schroeder, "Compact x-ray free-electron laser from a laser-plasma accelerator using a transverse-gradient undulator," *Phys. Rev. Lett.* **109**, p. 204801, Nov 2012.

[48] M. Fuchs, R. Weingartner, A. Popp, Z. Major, S. Becker, J. Osterhoff, I. Cortrie, B. Zeitler, R. Horlein, G. D. Tsakiris, U. Schramm, T. P. Rowlands-Rees, S. M. Hooker, D. Habs, F. Krausz, S. Karsch, and F. Gruner, "Laser-driven soft-x-ray undulator source," *Nat Phys* **5**(11), pp. 826–829, 2009.

[49] B. Hidding, S. Hooker, S. Jamison, B. Muratori, C. Murphy, Z. Najmudin, R. Pattathil, G. Sarri, M. Streeter, C. Welsch, *et al.*, "Plasma wakefield accelerator research 2019-2040: A community-driven uk roadmap compiled by the plasma wakefield accelerator steering committee (pwasc)," *arXiv preprint arXiv:1904.09205* , 2019.

[50] I. Gadjev, N. Sudar, M. Babzien, J. Duris, P. Hoang, M. Fedurin, K. Kusche, R. Malone, P. Musumeci, M. Palmer, I. Pogorelsky, M. Polyanskiy, Y. Sakai, C. Swinson, O. Williams, and J. B. Rosenzweig, "An inverse free electron laser acceleration-driven Compton scattering X-ray source," *Scientific Reports* **9**(532), 2019.

[51] F. Albert, S. G. Anderson, D. J. Gibson, C. A. Hagmann, M. S. Johnson, M. Messerly, V. Semenov, M. Y. Shverdin, B. Rusnak, A. M. Tremaine, F. V. Hartemann, C. W. Siders, D. P. McNabb, and C. P. J. Barty, "Characterization and applications of a tunable, laser-based, MeV-class Compton-scattering γ-ray source," *Physical Review Special Topics - Accelerators and Beams* **13**(7), pp. 1–13, 2010.

[52] S. G. Rykovanov, C. G. R. Geddes, J. L. Vay, C. B. Schroeder, E. Esarey, and W. P. Leemans, "Quasi-monoenergetic femtosecond photon sources from Thomson Scattering using laser plasma accelerators and plasma channels," *Journal of Physics B: Atomic, Molecular and Optical Physics* **47**(23), 2014.

[53] V. Petrillo, A. Bacci, R. Ben Alì Zinati, I. Chaikovska, C. Curatolo, M. Ferrario, C. Maroli, C. Ronsivalle, A. R. Rossi, L. Serafini, P. Tomassini, C. Vaccarezza, and A. Variola, "Photon flux and spectrum of γ-rays Compton sources," *Nuclear Instruments and Methods in Physics Research, Section A: Accelerators, Spectrometers, Detectors and Associated Equipment* **693**, pp. 109–116, 2012.

[54] E. Oz, S. Deng, T. Katsouleas, P. Muggli, C. D. Barnes, I. Blumenfeld, F. J. Decker, P. Emma, M. J. Hogan, R. Ischebeck, R. H. Iverson, N. Kirby, P. Krejcik, C. O'Connell, R. H. Siemann, D. Walz, D. Auerbach, C. E. Clayton, C. Huang, D. K. Johnson, C. Joshi, W. Lu, K. A. Marsh, W. B. Mori, and M. Zhou, "Ionization-induced electron trapping in ultrarelativistic plasma wakes," *Physical Review Letters* **98**(8), p. 084801, 2007.

[55] W. J. Brown and F. V. Hartemann, "Three-dimensional time and frequency-domain theory of femtosecond x-ray pulse generation through Thomson scattering," *Physical Review Special Topics - Accelerators and Beams* **7**(6), pp. 35–54, 2004.

[56] S. Wang, C. E. Clayton, B. E. Blue, E. S. Dodd, K. A. Marsh, W. B. Mori, C. Joshi, S. Lee, P. Muggli, T. Katsouleas, F. J. Decker, M. J. Hogan, R. H. Iverson, P. Raimondi, D. Walz, R. Siemann, and R. Assmann, "X-ray emission from betatron motion in a plasma wiggler," *Phys. Rev. Lett.* **88**, p. 135004, Mar 2002.

[57] S. Kiselev, A. Pukhov, and I. Kostyukov, "X-ray generation in strongly nonlinear plasma waves," *Phys. Rev. Lett.* **93**, p. 135004, Sep 2004.

[58] D. H. Whittum, "Electromagnetic instability of the ion-focused regime," *Physics of Fluids B: Plasma Physics* **4**(3), pp. 730–739, 1992.

[59] B. Ersfeld, R. Bonifacio, S. Chen, M. R. Islam, P. W. Smorenburg, and D. A. Jaroszynski, "The ion channel free-electron laser with varying betatron amplitude," *New Journal of Physics* **16**, p. 093025, sep 2014.

[60] M. Litos, R. Ariniello, C. Doss, K. Hunt-Stone, and J. R. Cary, "Experimental opportunities for the ion channel laser," *2018 IEEE Advanced Accelerator Concepts Workshop (AAC)* , pp. 1–5, 2018.